

Supplementary Information

Encapsulation of NiCo₂O₄ in nitrogen-doped reduced graphene oxide for sodium ion capacitors

Dongfang Yang,^a Qinglan Zhao,^a Liqing Huang,^b Binghui Xu,^c Nanjundan Ashok Kumar^a and X. S. Zhao^{a,c*}

^aSchool of Chemical Engineering, The University of Queensland, St Lucia, Brisbane 4072, Australia.

^bSchool of Mechanical and Mining Engineering, The University of Queensland, St Lucia, Brisbane 4072, Australia.

^cInstitute of Materials for Energy and Environment, Qingdao University, Qingdao 266071, China.

*Corresponding authors E-mail: george.zhao@uq.edu.au

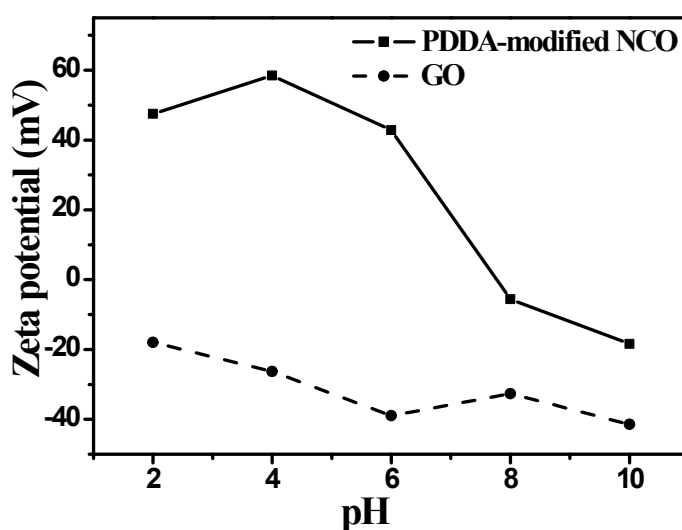


Fig. S1 Zeta potential profiles of PDDA-modified NCO and GO in the pH range between 2 and 10.

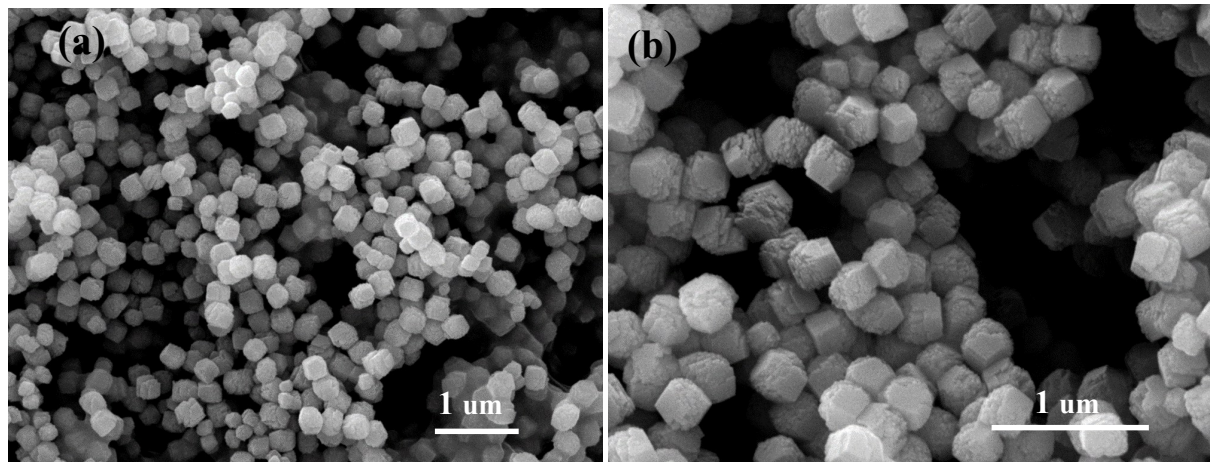


Fig. S2 SEM images of NCO particles.

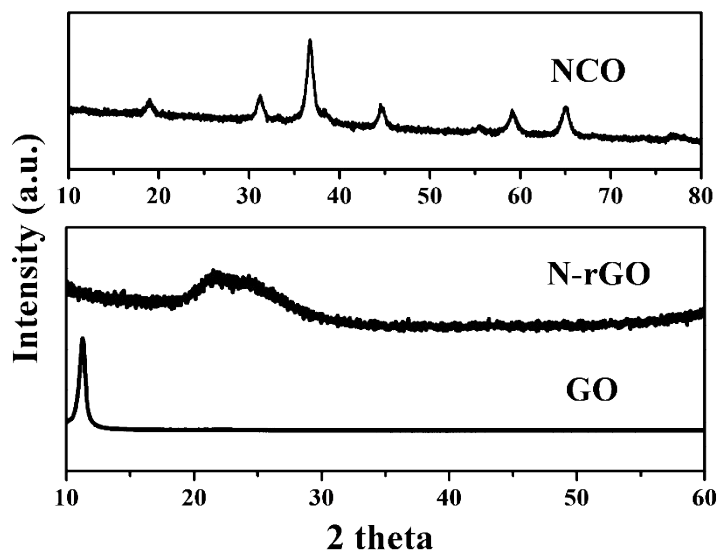


Fig. S3 XRD patterns of GO, N-rGO and NCO.

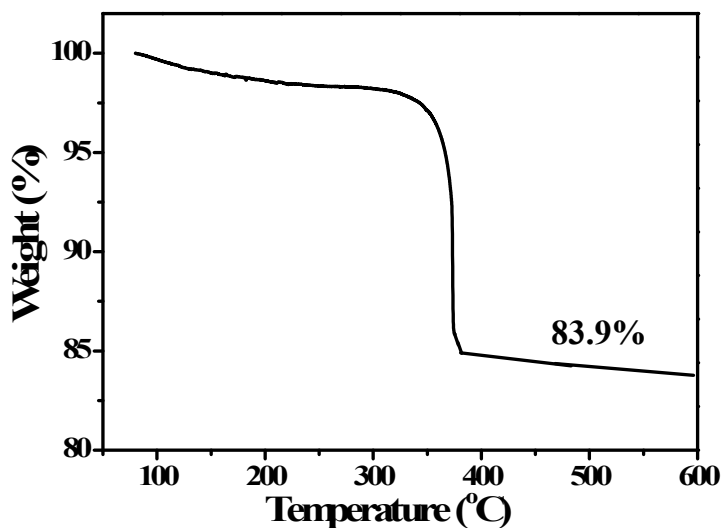


Fig. S4 Thermal gravimetric analysis (TGA) of NCO@N-rGO.

Table. S1 Fitting results of the EIS spectra in Fig. 3f using the inserted equivalent circuit.

Circuit element	NCO@N-rGO	NCO
R_c (Ω)	5.73	3.80
R_{ct} (Ω)	117	264
C_{ct} (nF)	690	902
W (mMho)	2.65	757

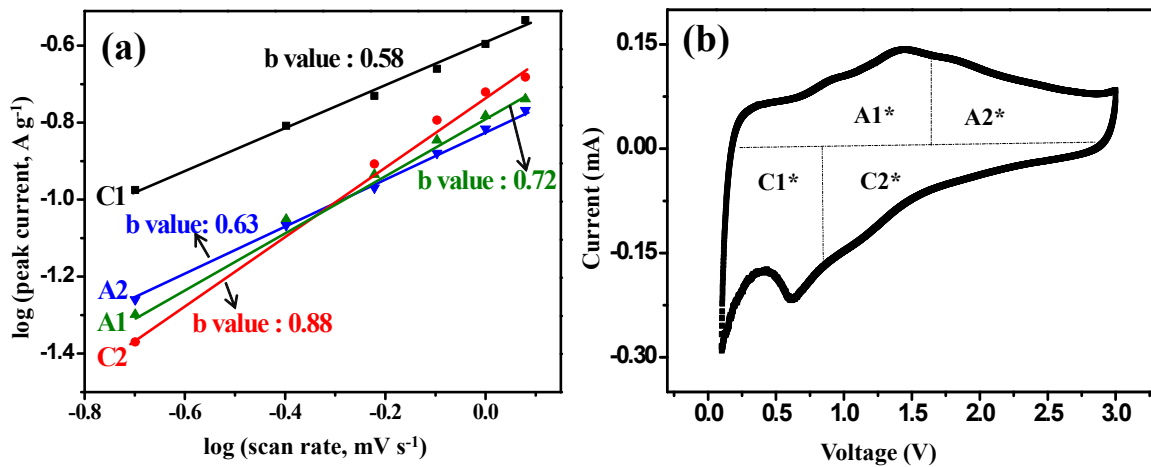


Fig. S5 (a) Peak current of NCO@N-rGO dependence on the scan rates from 0.2 to 1.2 mV s^{-1} , used to determine the b-values. (b) The CV curve of NCO@N-rGO at 1 mV s^{-1} , which was divided into four regions (C1^* , C2^* , A1^* and A2^*).

Table S2 Quantitative contributions of sodium ion storage via capacitive mechanism in the different regions defined in Fig. S5b.

Scan rate (mV s^{-1})	A1^*	A2^*	C1^*	C2^*
0.2	33.47%	24.14%	3.95%	76.05%
0.4	41.57%	31.03%	5.50%	81.79%
0.6	46.56%	35.53%	6.65%	84.62%
0.8	50.16%	38.89%	7.60%	86.40%
1	52.94%	41.57%	8.42%	87.66%
1.2	55.20%	43.80%	9.16%	88.61%